HHS Public Access

Author manuscript

Ann Occup Hyg. Author manuscript; available in PMC 2015 June 24.

Published in final edited form as:

Ann Occup Hyg. 2014 March ; 58(2): 182–194. doi:10.1093/annhyg/met053.

Effects of Breathing Frequency and Flow Rate on the Total Inward Leakage of an Elastomeric Half-Mask Donned on an Advanced Manikin Headform

Xinjian He[1], **Sergey A. Grinshpun**[1,*], **Tiina Reponen**[1], **Roy McKay**[1], **Michael S. Bergman**[2], and **Ziqing Zhuang**[2]

[1]Center for Health-Related Aerosol Studies, Department of Environmental Health, University of Cincinnati, 3323 Eden Avenue, Cincinnati, OH 45267, USA

[2]Technology Research Branch, National Personal Protective Technology Laboratory, National Institute for Occupational Safety and Health, 626 Cochrans Mill Road, Pittsburgh, PA 15236, USA

Abstract

Objectives—The objective of this study was to investigate the effects of breathing frequency and flow rate on the total inward leakage (TIL) of an elastomeric half-mask donned on an advanced manikin headform and challenged with combustion aerosols.

Methods—An elastomeric half-mask respirator equipped with P100 filters was donned on an advanced manikin headform covered with life-like soft skin and challenged with aerosols originated by burning three materials: wood, paper, and plastic (polyethylene). TIL was determined as the ratio of aerosol concentrations inside (C_{in}) and outside (C_{out}) of the respirator (C_{in}/C_{out}) measured with a nanoparticle spectrometer operating in the particle size range of 20–200 nm. The testing was performed under three cyclic breathing flows [mean inspiratory flow (MIF) of 30, 55, and 85 l/min] and five breathing frequencies (10, 15, 20, 25, and 30 breaths/min). A completely randomized factorial study design was chosen with four replicates for each combination of breathing flow rate and frequency.

Results—Particle size, MIF, and combustion material had significant ($P < 0.001$) effects on TIL regardless of breathing frequency. Increasing breathing flow decreased TIL. Testing with plastic aerosol produced higher mean TIL values than wood and paper aerosols. The effect of the breathing frequency was complex. When analyzed using all combustion aerosols and MIFs (pooled data), breathing frequency did not significantly ($P = 0.08$) affect TIL. However, once the data were stratified according to combustion aerosol and MIF, the effect of breathing frequency became significant ($P < 0.05$) for all MIFs challenged with wood and paper combustion aerosols, and for MIF = 30 l/min only when challenged with plastic combustion aerosol.

Conclusions—The effect of breathing frequency on TIL is less significant than the effects of combustion aerosol and breathing flow rate for the tested elastomeric half-mask respirator. The

*Author to whom correspondence should be addressed. Tel: +1-513-558-0504; fax: +1-513-558-2263; sergey.grinshpun@uc.edu.

DISCLAIMER

The findings and conclusions in this report are those of the authors and do not necessarily represent the views of the National Institute for Occupational Safety and Health (NIOSH). Mention of company names or products does not constitute endorsement by NIOSH.

greatest TIL occurred when challenged with plastic aerosol at 30 l/min and at a breathing frequency of 30 breaths/min.

Keywords

breathing frequency; combustion aerosol; flow rate; half-mask; manikin; total inward leakage

INTRODUCTION

The U.S. Occupational Safety and Health Administration (OSHA, 2006) requires respirators be provided to employees whenever engineering and work practice control measures are not adequate to reduce the employees' exposure to acceptable levels. Among the non-powered air-purifying respirators, filtering facepiece respirators (FFRs) are the most commonly used respiratory protection devices (share = 49%), followed by elastomeric half-masks (34%), according to the survey conducted in private industry by the U.S. Bureau of Labor Statistics and the National Institute for Occupational Safety and Health (BLS/NIOSH, 2003).

Smoke from a fire contains primarily ultrafine particles (<0.1 μm). The ultrafine particles were found to account for >70% of airborne particles (by number) measured in a large-scale fire test laboratory study (Baxter *et al.*, 2010). Exposure to ultrafine particles has been associated with impairment of cardiovascular function and other adverse health outcomes (Schwartz *et al.*, 1996; Peters *et al.*, 1997; Timonen *et al.*, 2005; Schulte *et al.*, 2008).

Many studies have evaluated the most penetrating particle size (MPPS) (Martin and Moyer, 2000; Grafe *et al.*, 2001; Bałazy *et al.*, 2006a, b; Eninger *et al.*, 2008; Rengasamy *et al.*, 2008; Cho *et al.*, 2010a) of NIOSH-certified N95 FFRs. These studies consistently report an MPPS in a range of 30–100 nm. Elastomeric half-masks, which offer the benefits of reusability, improved face seal, and enhanced user seal check capability—and can be decontaminated multiple times—(Roberge *et al.*, 2010), have not been studied as extensively as N95 FFRs. One study involving three half-masks and 10 FFRs tested on a panel of 10 human subjects concluded that the performance of elastomeric half-masks was better than that of FFRs (Han and Lee, 2005). Another study (Lawrence *et al.*, 2006) involving a panel of 25 subjects with varying face sizes reported superior performance of elastomeric N95 half-masks (15 models tested) over N95 FFRs (15 models tested) and surgical masks (6 models tested). However, these investigations used non-size-selective aerosol measurement devices that did not allow exploring potential differences in penetration by different particle sizes, and none of these investigations studied the effect of breathing frequency.

Respirator filter efficiency is significantly affected by breathing flow rate. This has been demonstrated for mechanical and "electret" filters tested under constant- and cyclic-flow conditions (Chen *et al.*, 1990; Brown, 1993; Qian *et al.*, 1998; Martin and Moyer, 2000; Bałazy *et al.*, 2006b; Huang *et al.*, 2007; Eninger *et al.*, 2008; Rengasamy *et al.*, 2008, 2009; Cho *et al.*, 2010b). A constant inhalation flow rate of 85 l/min is currently used in the NIOSH respirator certification program (NIOSH, 1995); however, constant flow does not accurately represent human breathing patterns. Stafford *et al.* (1973) reported that human breathing is more reasonably approximated by a sinusoidal waveform, which can be better

approximated with different flow rates and breathing frequencies (breaths/min) (Haruta *et al.*, 2008). Breathing frequency differs between population groups (e.g. healthy versus sick, young versus old) and is significantly affected by the level of physical activity (e.g. rest versus active) (Tortora and Anagnostakos, 1990; Sherwood, 2006). Several studies using cyclic flow have reported an effect of flow rate on filter efficiency and face seal leakage (Myers *et al.*, 1991; Eshbaugh *et al.*, 2008; Haruta *et al.*, 2008; Cho *et al.*, 2010b). However, with the exception of Wang *et al.* (2012), no published study has yet fully addressed the effect of the breathing frequency. Wang *et al.* (2012) did investigate two breathing frequencies (32 and 50 breaths/min) with a single mean inspiratory flow (MIF) (100 l/min), but the data generated in their study were too limited to draw conclusions about breathing frequency. Furthermore, they selected a breathing frequency (50 breaths/min) that is excessive for most workplace populations.

Respiratory protection offered by negative pressure respirators is dependent not only on the filter efficiency but also on face seal leakage (Zhuang *et al.*, 1998; Grinshpun *et al.*, 2009; Cho *et al.*, 2010b). To account for these two penetration pathways (filter and face seal leakage), NIOSH has proposed the total inward leakage (TIL) method for testing respirators (NIOSH/CDC, 2009). Several studies addressed this issue by creating artificial slit-like or circular leaks to assess the face seal leakage (Hinds and Bellin, 1987; Myers *et al.*, 1991; Chen and Willeke, 1992; Rengasamy and Eimer, 2011). However, artificial fixed leaks are not representative of actual conditions when a respirator is worn by humans. It is commonly assumed that size and location of face seal leaks constantly change during breathing, talking, and head/body movement (Myers *et al.*, 1996). Some studies tested respirators worn by human subjects (Zhuang *et al.*, 1998; Grinshpun *et al.*, 2009), but these were, obviously, limited to a non-toxic challenge aerosol (NaCl). Comprehensive testing of respirator performance in a toxic aerosol environment and at higher challenge concentrations requires use of a manikin headform. Conventional static manikin headforms (either made of a rigid material or coated with a thin layer of rubber, plastic, or other compressible materials) have been shown in the literature to have high TIL levels for half-mask elastomeric respirators and FFRs (Cooper *et al.*, 1983; Tuomi, 1985; Golshahi *et al.*, 2012). These older type headforms do not simulate the properties of human facial tissue (e.g. skin softness and local depth), which deforms under stress in ways that solid elastomers cannot simulate (Hanson and Priya, 2007). To address this gap, an advanced manikin headform was developed that is capable of mimicking the softness and thicknesses of the human skin (Hanson *et al.*, 2006; Bergman *et al.*, 2013).

Aiming at testing the performance of elastomeric half-mask respirators challenged with combustion aerosols, this study is a follow-up to recent studies (He *et al.*, 2013a,b) conducted in the same laboratory. The present study specifically addresses breathing frequency and flow rate as factors affecting TIL of an elastomeric half-mask respirator. The testing was conducted with respirators donned on an advanced headform that enables an adequate simulation of the human facial characteristics, which is crucial for measuring the TIL of a respirator. The advance manikin was challenged with three combustion aerosols: wood, paper, and plastic.

MATERIALS AND METHODS

Respirator

An elastomeric 3M 6000 series half-mask respirator equipped with two 3M 2091 P100 filters (3M Corp., St Paul, MN, USA) was chosen for the testing to assure the continuity of our previous research (He *et al.*, 2013a,b). The rationale for selecting the above respirator was described in detail by He *et al.* (2013a). An 11-mm-long flush probe with a 14-mm-diameter flange and a 4-mm-diameter inlet was mounted on the surface of the respirator centerline between the manikin's nose and upper lip. The end of the probe (14-mm flange) was flush with the interior surface of the half-mask. The probe was located ~25 mm from the manikin's nose/mouth.

Challenge aerosols

The challenge aerosols were separately generated by burning the following three materials inside a test chamber: wood (24-cm-long and 0.4-cm-diameter pellets, 1.9 ± 0.5 g), paper (23 × 24 cm brown multifold paper towel, 2.1 ± 0.2 g), and polyethylene (23 × 20 cm, 1.7 ± 0.3 g—further referred to as plastic) (He *et al.*, 2013a). Each material held by a caliper was ignited by a long-reach lighter and completely burnt inside the chamber. All burnt materials were captured in a water-filled basin placed on the floor. The measurements were initiated 15 min after burning to allow the combustion aerosol to reach a spatial uniformity. As our previous measurements revealed that 90% of particles so generated were within the range 20–200 nm (He *et al.*, 2013a), we focused on this size range.

Advanced manikin headform

The specifications of the advanced manikin headform chosen for this study were reported in detail by Bergman *et al.* (2013). Briefly, the headform is of the medium size defined by the NIOSH Principal Component Analysis panel created using data from a large-scale anthropometric survey of US workers conducted in 2003 (Zhuang *et al.*, 2007). A human-like skin with locally correct thicknesses was mounted on the headform skull. The material used to generate the skin is called Frubber™ (Hanson and White, 2004), a fluid-filled cellular matrix composed of an elastomer that compresses, elongates, and otherwise deforms in ways that simulates human skin (Hanson and White, 2004).

Experimental design and test conditions

The experimental setup is shown in Fig. 1. The respirator was donned on the advanced manikin headform, which was then challenged with one of three combustion aerosols (wood, paper, and plastic). The donning was performed according to the manufacturer's user instructions. After donning, the respirator was not redonned or repositioned until the completion of the study, which allowed maintaining the size and shape of the face seal leaks. Obviously, the static headform design did not allow fit testing of the respirator prior to the study. The P100 filters were changed after every 15 runs to minimize the effect of loading of combustion products on the filter medium. The filters were changed carefully to minimize the effect of this procedure on the respirator face seal leakage. After each filter change, the particle penetration was measured to assure that the size of the leak was consistent with the

one existing before the change under the same experimental conditions. Temperature and relative humidity were kept at 17–22°C and 30–50%, respectively.

The headform was connected to a Breathing Recording and Simulation System (BRSS, Koken Ltd, Tokyo, Japan) with a high-efficiency particulate air filter placed in between to keep particles from reentering the respirator cavity in exhaled air. The BRSS consists of an electromechanical drive-cylinder coupled with two air cylinders. As the electromechanical cylinder stroke moves back (inspiratory duration, half a period) and forth (expiratory duration, half a period), a sinusoidal air flow is generated (Haruta *et al.*, 2008). The stroke moving distance and frequency can be adjusted with a resolution of 0.1 mm and 0.01 Hz, respectively, thus allowing for precise changes to breathing flow rate and frequency when human breathing is simulated (Haruta *et al.*, 2008).

The test were conducted under three cyclic breathing flows (MIF—time weighted average flow rate over the width of an inspiration, MIF = 30, 55, and 85 l/min) and five breathing frequencies (10, 15, 20, 25, and 30 breaths/min). A completely randomized factorial study design was chosen with four replicates for each combination of the tested breathing flow rate and frequency. A summary of the experimental conditions is presented in Table 1. Aerosol concentrations inside (C_{in}) and outside (C_{out}) the respirator were measured using a nanoparticle spectrometer (Nano-ID NPS500, Naneum Ltd, Kent, UK) size selectively in 10 channels between 20 and 200 nm at a sampling flow rate of 0.2 l/min. Each concentration measurement took 3 min. The corresponding mean sizes for the 10 chosen channels were 22.4, 28.2, 35.5, 44.7, 56.2, 70.8, 89.1, 112.2, 141.3, and 177.8 nm. TIL was determined for each particle size (d_{p}) as the ratio of inside to outside concentration:

$$\text{TIL}_{d_{\text{p}}} = \frac{C_{\text{in},d_{\text{p}}}}{C_{\text{out},d_{\text{p}}}} \times 100\% \quad (1)$$

In addition, by combining the 10 channels, (overall) TIL was calculated for all combustion particles ranging from 20 to 200:

$$\text{TIL} = \frac{\sum_{i=1}^{10} N_{\text{in},i}}{\sum_{i=1}^{10} N_{\text{out},i}} \times 100\% \quad (2)$$

where N_{in} is the number of particles measured in a specific channel inside the respirator, N_{out} is the number of particles measured in a specific channel outside the respirator, and i is the ith particle size channel.

Data analysis

Data analysis was performed using SAS version 9.3 (SAS Institute Inc., Cary, NC, USA). For the size-selective TIL, the effect of particle size was analyzed using the one-way analysis of variance (ANOVA) on the pooled data. Three-way ANOVA was used to study the significance of combustion material, breathing flow, and breathing frequency for the

size-independent TIL. One-way ANOVA was performed to quantify the effect of breathing frequency on the size-independent TIL after stratifying the data by the combustion material and breathing flow. All pairwise comparisons were performed using Tukey's range test. *P*-values < 0.05 were considered significant.

RESULTS AND DISCUSSION

Size-selective TIL (TIL_{d_p})

The size-selective TIL values determined within the chosen 10-channel size range are shown in Fig. 2. The graphs represent three MIFs, five breathing frequencies, and three combustion aerosols (error bars are not shown as they make it difficult to see the data lines for each breathing frequency).

The reported TIL data were compared with the filter penetration data. The latter were obtained in our earlier study, which examined the performance of a fully sealed half-mask equipped with two P100 filters while challenged with wood, paper, and plastic combustion particles of size 20–200 nm (He *et al.*, 2013a). For most of the particle sizes, TIL was much greater than the filter penetration (<0.03%), suggesting that the face seal leakage was the primary particle penetration pathway for the tested elastomeric half-mask (an additional experiment was conducted to confirm that exhalation value did not leak).

The average size-selective TIL values obtained from this study were comparable to those reported in our previous study with a partially sealed (nose or nose–chin area) half-mask donned on a hard plastic manikin headform (He et al., 2013a,b), and 5- to 10-fold lower than those obtained with the unsealed half-mask donned on the plastic headform. This improvement can be attributed to the softness of the manikin skin, which deforms under stress, thus increasing the contact surface area and consequently forming a better seal.

Figure 2 shows that particle size affected TIL_{d_p} ($P < 0.0001$) only for particles <40 nm. For all three aerosols, the TIL_{d_p} values obtained at the lowest tested sizes, 20–40 nm, fell below those obtained at >40 nm regardless of the breathing flow and frequency. This can be explained by diffusional deposition, which is more pronounced for smaller particles (consequently, a smaller fraction could penetrate inside the respirator more readily). For particles 40–50 nm and larger, the TIL_{d_p} curves showed no consistent increasing or decreasing trend. Furthermore, ANOVA results showed no significant differences in TIL_{d_p} ($P = 0.36$) among the six channels between 45 and 200 nm. The relatively flat curves obtained for the half-mask indicate a wide range for the MPPS. No TIL MPPS data were available in the literature for elastomeric respirators until our recent study (He *et al.*, 2013a), which measured an MPPS of 120–140 nm for the same half-mask donned on a plastic manikin headform and challenged with plastic combustion aerosol. The cited study did not detect an MPPS for wood and paper aerosols due to multiple peaks in the TIL_{d_p} curves. Previous TIL studies have focused on N95 FFRs or surgical masks, for which the particle size effect was found significant and the TIL values were close to the penetration levels observed for the filters only (Myers *et al.*, 1991; Cho *et al.*, 2010a; Rengasamy and Eimer, 2011). At the same time, little information has been generated with respect to the MPPS for

face seal leakage. When testing N95 FFRs with artificially created cylindered leaks, Rengasamy and Eimer (2011) found that for leak diameters ≤1.65 mm, the MPPS was ~50 nm; we believe that this value likely represents the N95 filter penetration, whereas the TIL of the respirator used in this study (equipped with P100 filters) is primarily governed by the face seal leakage penetration. This likely explains the suppressed peaks or the plateaus seen in the curves presented in Fig. 2.

The effect of breathing frequency on TIL_{d_p} was complex. When challenged with wood combustion aerosol, frequencies of 30, 20, and 15 breaths/min produced the highest TIL_{d_p} values at MIF = 30, 55, and 85 l/min, for most size channels between 20 and 200 nm. MIF = 30 l/min produced the most notable effect of the breathing frequency on the TIL_{d_p}. The TIL_{d_p} curves obtained from testing with paper combustion aerosol showed some peaks at 30 and 10 breaths/min at MIF = 30 and 85 l/min, but no clear peak was identified for MIF = 55 l/min. The graphs representing TILs for plastic aerosol revealed separations between the TIL_{d_p} curves at MIF = 30 l/min, which essentially diminished at higher flow rates.

Increasing the MIF resulted in a decrease in the average TIL values for all challenge aerosols (wood, paper, and plastic). For example, for the wood combustion aerosol, the average TIL values were 0.6–1.0% at MIF = 30 l/min, 0.5–0.8% at 55 l/min, and 0.3–0.6% at 85 l/min. Several published FFR studies also reported that face seal penetration decreased with increase in breathing flow when challenged with particles >500 nm (Chen *et al.*, 1990; Cho *et al.*, 2010b). On the other hand, another FFR study observed no significant increase or decrease in face seal penetration by 8–400 nm particles associated with increasing breathing flow (Rengasamy and Eimer, 2011).

Size-independent (overall) TIL

The size-independent (overall) TIL values for the half-mask respirator challenged with the three tested combustion aerosols are presented in Fig. 3. The highest TIL values were determined at MIF = 30 l/min and 30 breaths/min for all three challenge aerosols (peak TIL = 1.08, 1.33, and 1.87% for wood, paper, and plastic, respectively). The lowest TIL values (0.35, 0.60, and 0.75% for wood, paper, and plastic, respectively) were obtained at MIF = 85 l/min combined with 25 breaths/min. ANOVA with Tukey's range test was performed to study the effects of combustion material, breathing flow, and breathing frequency on the TIL, and the data analysis results are presented in Tables 2 through 5.

Effect of the combustion aerosol—A three-way ANOVA (see Table 2) shows that the non-size-selective combustion aerosol significantly affected TIL ($P < 0.0001$). Pairwise multiple comparison analysis revealed that the mean overall TIL values for wood, paper, and plastic combustion aerosol were significantly ($P < 0.05$) different from each other (see Table 3). The plastic aerosol produced the highest mean TIL (1.14%) followed by wood (0.85%) and paper (0.70%). This finding is in agreement with our recent study (He *et al.*, 2013b) conducted with the same type of half-mask donned on a hard plastic manikin headform. The difference in TIL can be attributed to differences in particle shape, density, electric charge, and possibly other properties. Plastic (polyethylene) is pure hydrocarbon, paper is cellulose

(plus various additives and coatings), and wood is half cellulose and half lignin, which includes aromatics and relatively little hydrogen.

Effect of the breathing flow (MIF)—Breathing flow had a significant effect on TIL ($P < 0.0001$), as shown in Table 2. The interaction between the challenge aerosol and breathing flow (aerosol * MIF) was significant ($P = 0.0096$). The pairwise comparison results for three MIF groups (30, 55, and 85 l/min) are presented in Table 4. The mean TIL obtained at MIF = 30 l/min was significantly ($P < 0.05$) higher than those determined for MIF = 55 and 85 l/min. The differences between the data series obtained at 55 and 85 l/min were not significant ($P > 0.05$). One possible explanation is that a higher breathing flow can create a higher negative pressure inside the half-mask respirator, which sucks the respirator toward the manikin's face, thus creating tighter contact with the manikin headform (i.e. reducing face seal leakage). Increasing the flow rate from 30 to 55 l/min significantly reduced TIL; however, TIL was not significantly reduced from 55 to 85 l/min.

Effect of the breathing frequency—Breathing frequency did not show a significant effect on the TIL ($P > 0.05$, see Table 2) regardless of combustion aerosol, MIF, and breathing frequency (pooled data). When the data were stratified by combustion aerosol and MIF (see Table 5), the effect of the breathing frequency became significant ($P < 0.05$) for all conditions challenged with wood and paper combustion aerosols, and for MIF = 30 l/min only if challenged with plastic aerosol. However, no significant breathing frequency effect was found at MIF = 55 l/min ($P = 0.99$) and MIF = 85 l/min ($P = 0.97$) for plastic aerosol. The pairwise multiple comparisons confirmed that the frequency of 30 breaths/min produced the highest mean TIL value when MIF = 30 l/min, which was true for all three combustion aerosols (see Table 5). The findings were consistent with the results of size-selective TIL measurements (see Fig. 2). At MIF = 55 l/min, the highest mean TIL values were recorded at 20 breaths/min for wood combustion aerosol (TIL = 0.89%) and at 30 breaths/min for paper aerosol (TIL = 0.88%); no peak TIL value was observed for plastic aerosol. For the MIF = 85 l/min, the highest mean TIL values were recorded at 15 breaths/min for wood combustion aerosol (TIL = 0.67%) and at 10 breaths/min for paper aerosol (TIL = 0.90%); again, no peak TIL value was found for plastic aerosol.

In summary, the data suggest that the breathing frequency effect is rather complex and dependent on the combustion aerosol and MIF. It is concluded that the breathing frequency affects the TIL less than factors such as combustion aerosol and breathing flow rate. This finding points to the importance of a proper selection of challenge aerosol and MIF when testing the performance of the elastomeric half-mask respirators. Nevertheless, for a certain chosen aerosol and MIF, different breathing frequencies can produce significant differences among the TIL values. For example, for wood aerosol and MIF = 30 l/min, the highest TIL (1.08%) obtained at 30 breaths/min was almost 1.5-fold higher than the one (0.74%) obtained at 15 breaths/min. At MIF = 85 l/min, the highest TIL found for the wood aerosol (0.67% at 15 breaths/min) was almost twice greater than the lowest TIL (0.35% at 25 breaths/min). In addition to characterizing the role of breathing frequency in the performance evaluation of an elastomeric respirator, the findings of this study support testing with cyclic flow (the present NIOSH certification protocol utilizes the constant-flow

condition). A similar conclusion was made for other types of respirators (Eshbaugh *et al.*, 2008; Haruta *et al.*, 2008; Grinshpun *et al.*, 2009).

A limitation of the study is that only one model of elastomeric half-mask respirators was tested. Generally, the results may differ from one model to another. In addition, only a single donning was conducted so that a contaminated respirator would not be subjected to a replicate testing. It remains unknown how the results would differ given that the respirator model characteristics and between-donning variability may cause leaks of different sizes and shapes. While we believe that the major trends would remain the same, it seems meaningful to expand the present study in the future involving alternative experimental designs and other half-mask models as well as, possibly, other classes of respirators (i.e. full facepiece and FFRs).

CONCLUSIONS

Breathing flow and combustion material had significant ($P < 0.001$) effects on the TIL regardless of the level of the breathing frequency. The particle size effect on the TIL was not significant ($P = 0.36$) for particles >40 nm. The relatively flat curves generated in the size-selective experiments between ~40 and 200 nm serve as an evidence of a wide size range of particles, which most readily penetrate through face seal leaks of half-mask respirators.

The effect of the breathing frequency was complex and differed for different combinations of the combustion aerosol and the MIF. For pooled data, the breathing frequency had no significant ($P = 0.08$) effect on the non-size-selective TIL. However, after stratifying the data according to combustion aerosol and MIF, the breathing frequency effect became significant ($P < 0.05$) for all MIFs when challenged with wood and paper combustion aerosols, and specifically for MIF = 30 l/min when challenged with plastic aerosol. More studies are needed to fully understand the effect of breathing frequency.

Plastic aerosols produced higher overall mean TIL values ($P < 0.05$) compared with wood and paper aerosols, suggesting potentially higher exposure to a wearer. The highest penetration occurred when challenged with plastic aerosol, at 30 l/min, and at a breathing frequency of 30 breaths/min. The results also showed that an increase in the MIF leads to a decrease in TIL, a trend that lost its significance as the flow rate exceeded 55 l/min. In summary, the results suggest that when testing respirators on breathing manikins, a flow rate (not a breathing frequency) should be considered as a primary breathing characteristic to be addressed. The TIL results also indicate that for particles >40 nm, the particle size effect was not significant, and particles <40 nm produced lower penetration than those >40 nm. This finding suggests that size-selective measurement may not be necessary when performing the TIL test.

Acknowledgments

The BRSS was made available thanks to courtesy of Koken Ltd (Tokyo, Japan). The authors are grateful to Dr Joseph Wander who provided numerous valuable comments to the draft of this manuscript.

FUNDING

National Institute for Occupational Safety and Health Targeted Research Training Program and Pilot Research Project Training Program (University of Cincinnati, Education and Research Center, Grant T42/OH008432-07).

References

Bałazy A, Toivola M, Adhikari A, et al. Do N95 respirators provide 95% protection level against airborne viruses, and how adequate are surgical masks? Am J Infect Control. 2006a; 34:51–7. [PubMed: 16490606]

Bałazy A, Toivola M, Reponen T, et al. Manikin-based performance evaluation of N95 filtering-facepiece respirators challenged with nanoparticles. Ann Occup Hyg. 2006b; 50:259–69. [PubMed: 16344291]

Baxter CS, Ross CS, Fabian T, et al. Ultrafine particle exposure during fire suppression-is it an important contributory factor for coronary heart disease in firefighters? J Occup Environ Med. 2010; 52:791–6. [PubMed: 20657302]

Bergman MS, Zhuang Z, Wander J, et al. Development of an advanced respirator fit test headform. J Occup Environ Hyg. 201310.1080/15459624.2013.816434

BLS/NIOSH. Respirator usage in private sector firms, 2001. U.S Department of Labor, Bureau of Labor Statistics/U.S. Department of Health and Human Services, Public Health Service, Centers for Disease Control and Prevention, National Institute for Occupational Safety and Health; 2003.

Brown, RC. Air filtration: an integrated approach to the theory and applications of fibrous filters. Oxford: Pergamon Press; 1993. p. 109

Chen CC, Ruuskanen J, Pilacinski W, et al. Filter and leak penetration characteristics of a dust and mist filtering facepiece. Am Ind Hyg Assoc J. 1990; 51:632–9. [PubMed: 2270830]

Chen CC, Willeke K. Characteristics of face seal leakage in filtering facepieces. Am Ind Hyg Assoc J. 1992; 53:533–9. [PubMed: 1524028]

Cho KJ, Jones S, Jones G, et al. Effect of particle size on respiratory protection provided by two types of N95 respirators used in agricultural settings. J Occup Environ Hyg. 2010a; 7:622–7. [PubMed: 20835946]

Cho KJ, Reponen T, McKay R, et al. Large particle penetration through N95 respirator filters and facepiece leaks with cyclic flow. Ann Occup Hyg. 2010b; 54:68–77. [PubMed: 19700488]

Cooper DW, Hinds WC, Price JM, et al. Common materials for emergency respiratory protection: leakage tests with a manikin. Am Ind Hyg Assoc J. 1983; 44:720–6. [PubMed: 6650392]

Eninger RM, Honda T, Adhikari A, et al. Filter performance of N99 and N95 facepiece respirators against viruses and ultrafine particles. Ann Occup Hyg. 2008; 52:385–96. [PubMed: 18477653]

Eshbaugh JP, Gardner PD, Richardson AW, et al. N95 and P100 respirator filter efficiency under high constant and cyclic flow. J Occup Environ Hyg. 2008; 6:52–61. [PubMed: 19012163]

Golshahi L, Telidetzki K, King B, et al. A pilot study on the use of geometrically accurate face models to replicate ex vivo N95 mask fit. Am J Infect Control. 2012; 41:77–9. [PubMed: 22503133]

Grafe, T.; Gogins, M.; Barris, M., et al. Nanofibers in filtration applications in transportation. Filtration 2001 Conference Proceedings; Chicago, IL. 2001. p. 1-15.

Grinshpun SA, Haruta H, Eninger RM, et al. Performance of an N95 filtering facepiece particulate respirator and a surgical mask during human breathing: two pathways for particle penetration. J Occup Environ Hyg. 2009; 6:593–603. [PubMed: 19598054]

Han D-H, Lee J. Evaluation of particulate filtering respirators using inward leakage (IL) or total inward leakage (TIL) testing—Korean experience. Ann Occup Hyg. 2005; 49:569–74. [PubMed: 16126767]

Hanson, D.; Bergs, R.; Tadesse, Y., et al. Enhancement of EAP actuated facial expressions by designed chamber geometry in elastomers. Proc SPIE's Electroactive Polymer Actuators and Devices Conf., 10th Smart Structures and Materials Symposium; San Diego, CA. 2006.

Hanson, D.; Priya, S. NSF Phase 1 Final Report. National Science Foundation STTR award, NSF 05-557; 2007. An actuated skin for robotic facial expressions.

Hanson, D.; White, V. Converging the capabilities of electroactive polymer artificial muscles and the requirements of bio-inspired robotics. Proc SPIE's Electroactive Polymer Actuators and Devices Conf., 10th Smart Structures and Materials Symposium; San Diego, CA. 2004.

Haruta H, Honda T, Eninger RM, et al. Experimental and theoretical investigation of the performance of N95 respirator filters against ultrafine aerosol particles tested at constant and cyclic flows. J Int Soc Resp Prot. 2008; 25:75–88.

He X, Grinshpun SA, Reponen T, et al. Laboratory evaluation of the particle size effect on the performance of an elastomeric half-mask respirator against ultrafine combustion particles. Ann Occup Hyg. 2013a10.1093/annhyg/met014

He X, Yermakov M, Reponen T, et al. Manikin-based performance evaluation of elastomeric respirators against combustion particles. J Occup Environ Hyg. 2013b; 10:203–12. [PubMed: 23442086]

Hinds WC, Bellin P. Performance of dust respirators with facial seal leaks: II. Predictive model. Am Ind Hyg Assoc J. 1987; 48:842–7. [PubMed: 3318364]

Huang S-H, Chen C-W, Chang C-P, et al. Penetration of 4.5 nm to aerosol particles through fibrous filters. J Aerosol Sci. 2007; 38:719–27.

Lawrence RB, Duling MG, Calvert CA, et al. Comparison of performance of three different types of respiratory protection devices. J Occup Environ Hyg. 2006; 3:465–74. [PubMed: 16857645]

Martin SB, Moyer ES. Electrostatic respirator filter media: filter efficiency and most penetrating particle size effects. Appl Occup Environ Hyg. 2000; 15:609–17. [PubMed: 10957816]

Myers WR, Kim H, Kadrichu N. Effect of particle size on assessment of faceseal leakage. J Int Soc Resp Prot. 1991; 9:6–21.

Myers WR, Zhuang Z, Nelson T. Field performance measurements of half-facepiece respirators – foundry operations. Am Ind Hyg Assoc J. 1996; 57:166–74. [PubMed: 8615325]

NIOSH. Fed Reg. Vol. 60. National Institute for Occupational Safety and Health. US DHHS, Public Health Service; 1995. Respiratory protective devices; final rules and notices; p. 30335-93.

NIOSH/CDC. National Institute for Occupational Safety and Health. Washington, DC: US DHHS, Public Health Service; 2009. Total inward leakage for half-mask air-purifying respirators.

OSHA. Respirator protection, 29 CFR 1910.134. Washington, DC: Occupational Safety & Health Administration; 2006.

Peters A, Wichmann HE, Tuch T, et al. Respiratory effects are associated with the number of ultrafine particles. Am J Respir Crit Care Med. 1997; 155:1376–83. [PubMed: 9105082]

Qian Y, Willeke K, Grinshpun SA, et al. Performance of N95 respirators: filtration efficiency for airborne microbial and inert particles. Am Ind Hyg Assoc J. 1998; 59:128–32. [PubMed: 9487666]

Rengasamy S, Eimer BC. Total inward leakage of nanoparticles through filtering facepiece respirators. Ann Occup Hyg. 2011; 55:253–63. [PubMed: 21292731]

Rengasamy S, Eimer BC, Shaffer RE. Comparison of nanoparticle filtration performance of NIOSH-approved and CE-marked particulate filtering facepiece respirators. Ann Occup Hyg. 2009; 53:117–28. [PubMed: 19261695]

Rengasamy S, King WP, Eimer BC, et al. Filtration performance of NIOSH-approved N95 and P100 filtering facepiece respirators against 4 to 30 nanometer-size nanoparticles. J Occup Environ Hyg. 2008; 5:556–64. [PubMed: 18607812]

Roberge RJ, Coca A, Williams WJ, et al. Reusable elastomeric air-purifying respirators: physiologic impact on health care workers. Am J Infect Control. 2010; 38:381–6. [PubMed: 20189685]

Schulte P, Geraci C, Zumwalde R, et al. Occupational risk management of engineered nanoparticles. J Occup Environ Hyg. 2008; 5:239–49. [PubMed: 18260001]

Schwartz J, Dockery DW, Neas LM. Is daily mortality associated specifically with fine particles? J Air Waste Manage Assoc. 1996; 46:927–39.

Sherwood, L. Fundamentals of physiology: a human perspective. Belmont, CA: Thomson Brooks/Cole; 2006. p. 380

Stafford RG, Ettinger HJ, Rowland TJ. Respirator cartridge filter efficiency under cyclic- and steady-flow conditions. Am Ind Hyg Assoc J. 1973; 34:182–92. [PubMed: 4517069]

Timonen KL, Vanninen E, de Hartog J, et al. Effects of ultrafine and fine particulate and gaseous air pollution on cardiac autonomic control in subjects with coronary artery disease: the ULTRA study. J Expos Sci Environ Epidemiol. 2005; 16:332–41.

Tortora, GJ.; Anagnostakos, NP. Principles of anatomy and physiology. 6. New York, NY: Harper-Collins; 1990. p. 707

Tuomi T. Face seal leakage of half-masks and surgical masks. Am Ind Hyg Assoc J. 1985; 46:308–12. [PubMed: 4014006]

Wang A, Richardson AW, Hofacre KC. The effect of flow pattern on collection efficiency of respirator filters. J Int Soc Resp Prot. 2012; 29:41.

Zhuang Z, Coffey CC, Myers WR, et al. Quantitative fittesting of N95 respirators: part I-method development. Int Soc Resp Prot. 1998; 16:11–24.

Zhuang ZQ, Bradtmiller B, Shaffer RE. New respirator fit test panels representing the current US civilian work force. J Occup Environ Hyg. 2007; 4:647–59. [PubMed: 17613722]

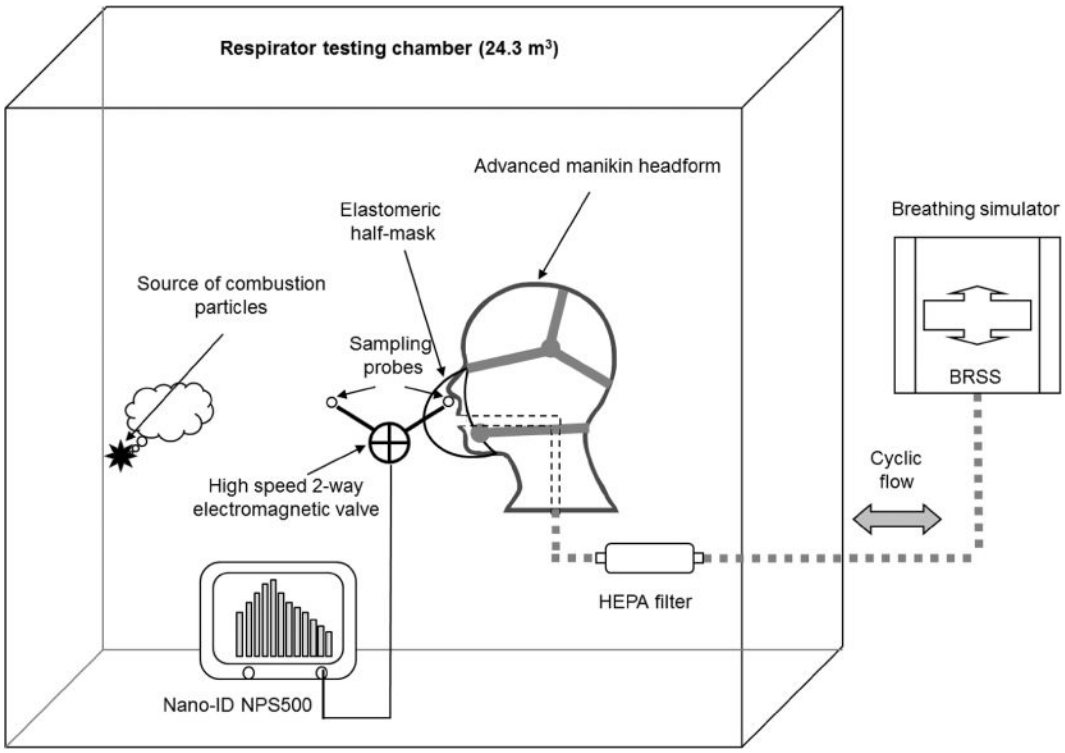

Figure 1.
Schematic diagram of the experimental setup (modified from He *et al.*, 2013a).

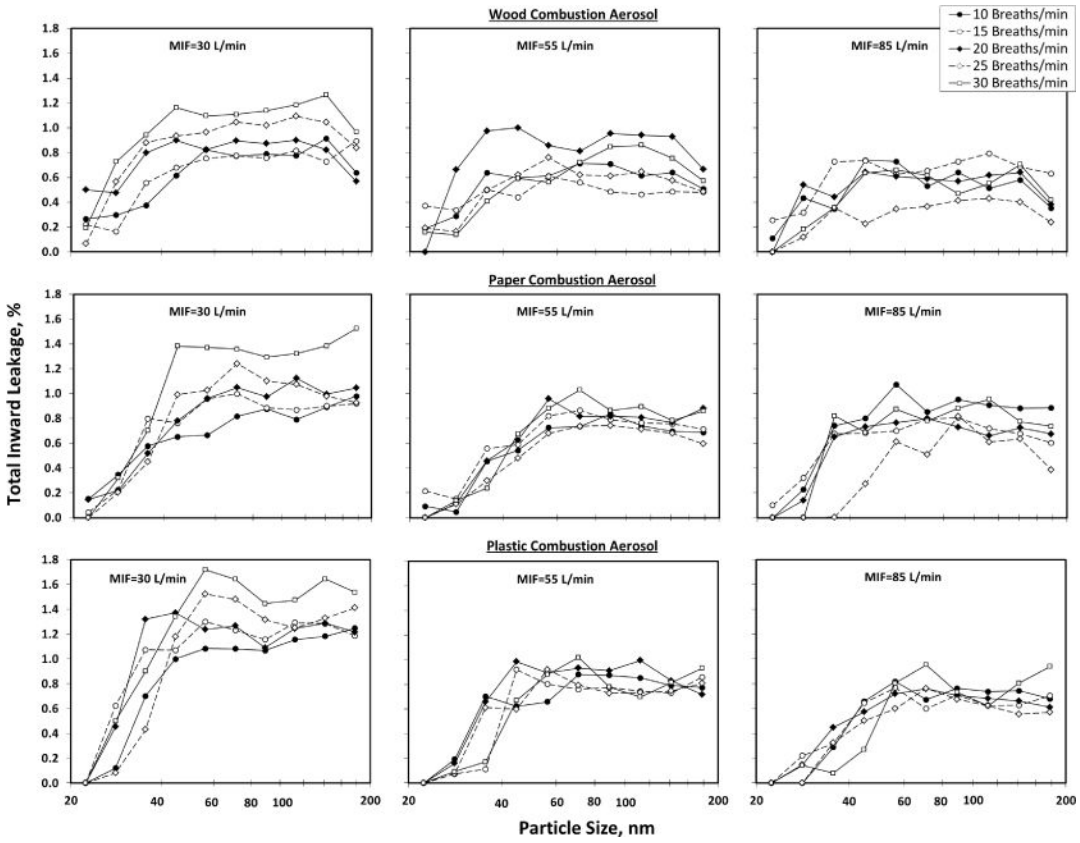

Figure 2.

Size-selective TIL values for an elastomeric half-mask respirator donned an advanced manikin headform while challenged with three combustion aerosols (wood, paper, and plastic). Each point represents the average value of four replicates.

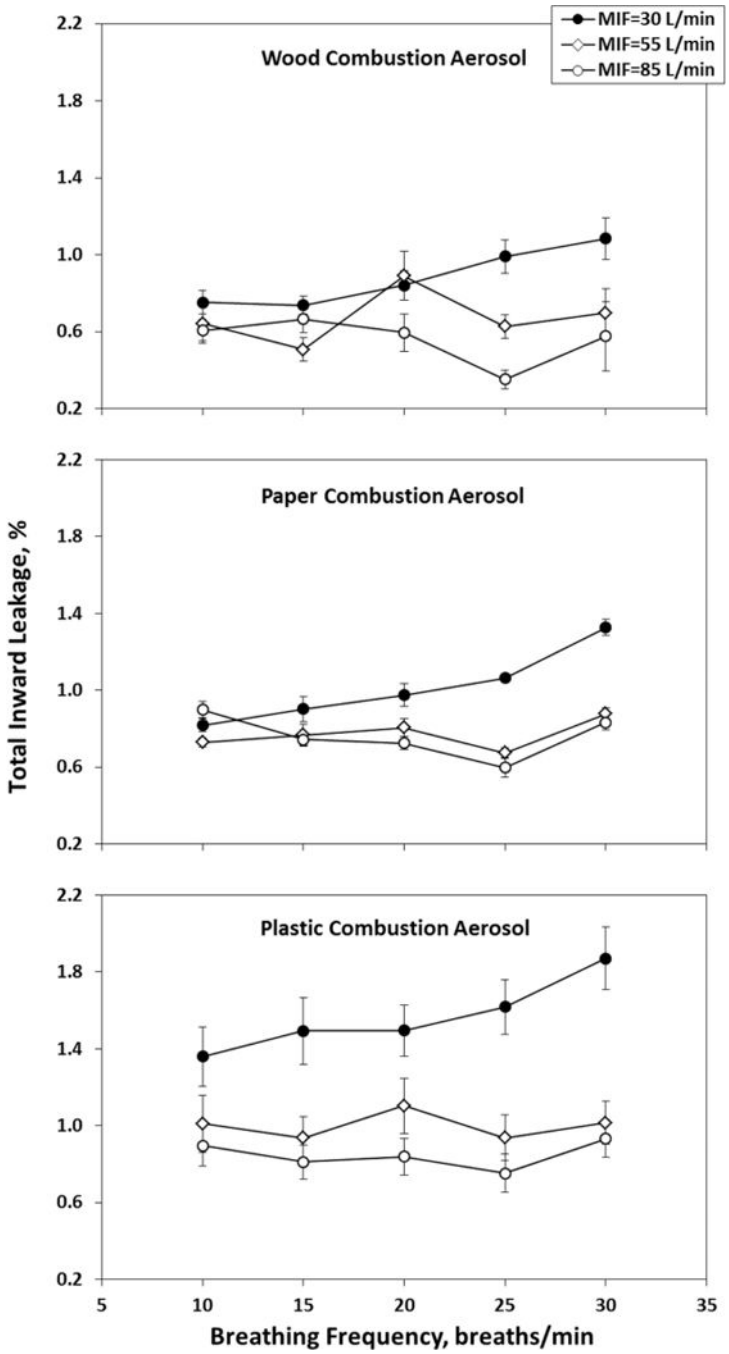

Figure 3.

Size-independent (overall) TIL values for an elastomeric half-mask respirator donned an advanced manikin headform while challenged with three combustion aerosols (wood, paper, and plastic). Each point represents the average value of four replicates after combining all the channels between 20 and 200 nm, and the error bar represents the standard error of the mean.

Table 1

Summary of the experimental conditions

Variable	Levels
Respirator type	One elastomeric half-mask with P100 filters (medium size, 3M 6000 series)
Challenge aerosol	Paper, wood, and plastic combustion aerosols
Breathing flow rate	Cyclic 30, 55, and 85 l/min
Breathing frequency	10, 15, 20, 25, and 30 breaths/min
Particle size range	20–200 nm (10 channels)
Replicates	4
Total runs:	3 × 3 × 5 × 4 = 180

Table 2

Three-way ANOVA results for the size-independent (overall) TIL as a function of combustion aerosol, MIF, and breathing frequency

Source	DF	ANOVA SS	Mean square	*F*-value	*P*-value
Aerosol	2	5.81	2.90	28.40	<0.0001
MIF	2	6.24	3.12	30.49	<0.0001
Aerosol * MIF	4	1.43	0.35	3.49	0.0096
Bf	4	0.86	0.21	2.10	0.0841
Aerosol * Bf	8	0.09	0.01	0.12	0.9983
MIF * Bf	8	1.38	0.17	1.68	0.1076
Aerosol * MIF * Bf	16	0.23	0.01	0.14	1.0000

Bf, breathing frequency; DF, degrees of freedom; SS, sum of squares. Three-way ANOVA were performed on all levels of combustion aerosol, MIF, and Bf (pooled data).

The asterisk (*) indicates an interaction between variables.

Table 3

Pairwise multiple comparisons: mean TIL values among three combustion aerosol groups (ANOVA with Tukey's range test)

Tukey grouping[a]	Mean[b] TIL (%)	Aerosol
A	1.14	Plastic
B	0.85	Paper
C	0.70	Wood

[a] Means with the same letter are not significantly different (*P*-value > 0.05).

[b] Calculated using the size-independent (overall) TIL values.

Table 4

Pairwise multiple comparisons: mean TIL values among three MIF groups (ANOVA with Tukey's range test)

Tukey grouping[a]	Mean[b] TIL (%)	MIF (l/min)
A	1.15	30
B	0.81	55
B	0.72	85

[a] Means with the same letter are not significantly different (P-value > 0.05).

[b] Calculated using the size-independent (overall) TIL values.

Table 5

Pairwise multiple comparisons: mean TIL values among five breathing frequency groups challenged with combustion aerosols (ANOVA with Tukey's range test)

Wood combustion aerosol				Paper combustion aerosol				Plastic combustion aerosol			
Tukey grouping[a]	Mean[b] TIL (%)	Breathing frequency (breaths/min)	*P*-value[c]	Tukey grouping[a]	Mean[b] TIL (%)	Breathing frequency (breaths/min)	*P*-value[c]	Tukey grouping[a]	Mean[b] TIL (%)	Breathing frequency (breaths/min)	*P*-value[c]
MIF = 30 l/min			0.0265	MIF = 30 l/min			<0.0001	MIF = 30 l/min			0.0476
A	1.08	30		A	1.33	30		A	1.87	30	
A B	0.99	25		B	1.06	25		A B	1.62	25	
A B	0.84	20		B C	0.97	20		A B	1.50	20	
B	0.75	10		C D	0.90	15		A B	1.49	15	
B	0.74	15		D	0.82	10		B	1.36	10	
MIF = 55 l/min			0.0373	MIF = 55 l/min			0.0231	MIF = 55 l/min			0.9890
A	0.89	20		A	0.88	30		A	1.10	20	
A	0.70	30		A B	0.81	20		A	1.01	30	
A B	0.64	10		B C	0.77	15		A	1.01	10	
A B	0.63	25		B C	0.73	10		A	0.94	15	
B	0.51	15		C	0.67	25		A	0.94	25	
MIF = 85 l/min			0.0391	MIF = 85 l/min			0.0260	MIF = 85 l/min			0.9689
A	0.67	15		A	0.90	10		A	0.93	30	
A	0.61	10		A B	0.83	30		A	0.90	10	
A	0.60	20		A B	0.74	15		A	0.84	20	
A	0.58	30		B	0.73	20		A	0.81	15	
B	0.35	25		B	0.72	25		A	0.75	25	

[a] Within each group of the combustion aerosol (wood, paper, and plastic), means with the same letter are not significantly different (*P*-value > 0.05).

[b] Calculated using the size-independent (overall) TIL values.

[c] *P*-values were obtained from the one-way ANOVA performed to examine the effect of the breathing frequency on the size-independent TIL after stratifying the combustion aerosol and the MIF.